

# Sensitivity Analysis of Side Slip Angle for a Front Wheel Steering Vehicle : a Frequency Domain Approach

Jin-Hee Jang\* and Chang-Soo Han\*\*

(Received February 1, 1996)

In this paper, sensitivity analysis of side slip angle for a front wheel steering vehicle is performed in the frequency domain. For the derivation of the transfer function, a simple vehicle model with two degrees of freedom is used in the initial modeling stage. This model exhibits the simplest lateral dynamic effect, and is useful for understanding the dynamic characteristics and control aspects of the target system. Vehicle mass, inertia, cornering stiffness, and wheel base are taken to be the design variables. Sensitivity functions of the transfer function with respect to the design variables are derived. From this study, we see that a transition speed exists in the frequency response of side slip angle. This implies that the characteristics are changed from minimum phase to non-minimum phase as the vehicle speed increases. The objective of this study is to propose a basis for design and re-design of the vehicle by checking the side slip angle variations with respect to design variable changes in the frequency domain. Finally, dominant design variables are suggested based on the sensitivity analysis.

**Key Words:** Sensitivity Analysis, Lateral Vehicle Dynamics, Side Slip Angle, Steering Characteristics, Transition Speed, Non-Minimum Phase

## Nomenclature

- $m$  : Vehicle mass  
 $I$  : Moment of inertia of a vehicle in yaw direction  
 $V$  : Vehicle speed  
 $K_f$  : Cornering stiffness of a front wheel  
 $K_r$  : Cornering stiffness of a rear wheel  
 $l_f$  : Distance from c. g. to front wheel center  
 $l_r$  : Distance from c. g. to rear wheel center  
 $\delta_f$  : Front wheel steering angle

## 1. Introduction

Sensitivity analysis is an efficient tool for checking the effects of the design variables on the system state variables (Deif, 1986). State variables represent dynamic characteristics of the system,

while, design variables are specified from the design criteria. Therefore, characteristics of state variables are governed by the initial values of design variables. In the case of re-designing a system, sensitivity information can be used as a design basis (Vanderplaats, 1984; Arora, 1989), so that sensitivity analysis is an important tool for the designer.

This is classified by static, kinematic, and dynamic sensitivity analysis with respect to system state. Static sensitivity analysis is used to check the variations of the state variables with respect to design variable changes in the static state. Particularly, this can be utilized in structural design. The kinematic sensitivity analysis can be applied to the kinematic state of the mechanism (Haug and Sohoni, 1984). Dynamic sensitivity analysis is utilized for evaluation of the variation of the target mechanism in the dynamic state (Krishnaswami *et al.*, 1983, Haug *et al.*, 1984, Chang and Nikraves, 1985, Jang and Han, 1995).

\* Dept. of Precision Mechanical Engineering, Graduate School of Hanyang Univ.

\*\* Dept. of Mechanical Engineering, Hanyang Univ.

This sensitivity analysis is based on the time domain approach. But, for evaluation of the steady state characteristics of the target system, frequency domain analysis is necessary. A sensitivity analysis of the yaw rate of a front wheel steering vehicle in the frequency domain was performed by Jang and Han (1997). From this research, we see that the frequency response of the yaw rate is always stable. This means that the response has minimum phase characteristics owing to the stable zero dynamics (Jang and Han, 1997).

In this paper, sensitivity analysis of the side slip angle of the front wheel steering vehicle is considered in the frequency domain. The lateral vehicle dynamics are involved in steering maneuver when an automobile is driven at various speeds. Generally, the steering maneuver of the vehicle is carried out by the steering wheel input of the driver. The vehicle is then steered to the desired target path of the driver. This is one of the important maneuvers for the maneuverability of the vehicle (Whitehead, 1988). Front wheel steering vehicle is common in most passenger cars.

In order to study the sensitivity analysis of side slip angle and check the validity of the developed control logic, a simple bicycle model is widely used. It can also be used for evaluation of the basic lateral dynamic response (Ellis, 1969; Gillespie, 1992; Shiotsuka, Nagamatsu, and Yoshida, 1993). This model is the simplest possible for the verification of some types of steering maneuver (Jansen and van Oosten, 1994). The second candidate is a lumped multi-degree of freedom vehicle model. The entire vehicle is modeled by a mass, spring, and damper. This is the intermediate form of the vehicle model for steering and suspension system effect. The last form of the vehicle model is a multi-body vehicle model consisting of mass, spring, damper, and any mechanical joints. It is useful for examination of the more detail vehicle characteristics such as three dimensional mechanical information (Jang *et al.*, 1995)

In the steering maneuvers of the front wheel steering vehicle, two dominant state variables, side slip angle and yaw rate, are conventionally used. In this paper, side slip angle response in the

frequency domain is studied. For this purpose, a transfer function and some useful basic terms ( $SF$ ,  $\zeta$ , and  $\omega_n$ ) are defined and used to understand the steady state characteristics of the vehicle. These terms are also used for formulation of the sensitivity functions. Magnitude and phase response are evaluated, and sensitivity results of the response are suggested by these derived sensitivity functions. All formulations for the sensitivity analysis are performed by first order partial differentiation with respect to the design variables.

The objective of this research is to determine sensitivity information for the magnitude and phase of the side slip angle with respect to the design variable change. Finally, for re-design and initial design of the vehicle, dominant design variables of the system are suggested based on the analyses in the frequency domain.

## 2. Vehicle Modeling

Although various vehicle models can be used for our purposes, a simple bicycle vehicle model is selected for the analytical derivation of the sensitivity equations with respect to some design variables. A vehicle in steering is represented in Fig. 1 and the major concern is regarding the lateral vehicle dynamics in steering maneuver.

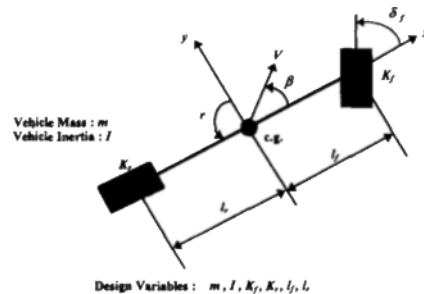


Fig. 1 A vehicle in steering maneuver

Each parameter and design variable is listed in the nomenclature. The side slip angle and yaw rate are selected as the state variables of the system as follows:

$$\underline{z} = [\beta \ r]^T \quad (1)$$

where  $\underline{z}$  is the state variable vector,  $\beta$  is side slip angle, and  $r$  represents the yaw rate of the vehicle obvious. Design variables of this system are selected as the following:

$$\begin{aligned} \underline{b} &= [b_1 \ b_2 \ b_3 \ b_4 \ b_5 \ b_6]^T \\ &= [m \ I \ K_f \ K_r \ l_f \ l_r]^T \end{aligned} \quad (2)$$

The governing mathematical equations of motion for the front wheel steering vehicle can be expressed as in Eqs. (3) and (4) (Jang, 1995a). These equations can be derived with the assumption that side slip angle is very small, and the cornering stiffness ( $K_f$  and  $K_r$ ) has linear characteristics under normal driving conditions. Also, weight transfer between the right and the left of the vehicle, as well as the effects of the vehicle width, are ignored.

$$mV \frac{d\beta}{dt} + 2(K_f + K_r) \beta + \left[ mV + \frac{2}{V} (l_f K_f - l_r K_r) \right] = 2K_r \delta_f \quad (3)$$

$$2(l_f K_f - l_r K_r) \beta + I \frac{dr}{dt} + \left[ \frac{2(l_f^2 K_f + l_r^2 K_r)}{V} \right] r = 2l_f K_f \delta_f \quad (4)$$

Equations (3) and (4) are the basic equations for two dimensional plane motion of the vehicle. The left sides of Eqs. (3) and (4) represent motion of the vehicle, and the right sides of the equation are inputs to the vehicle, with front wheel steering angle ( $\delta_f$ ). From Eqs. (3) and (4), taking Laplace transforms of each side, we obtain the following equations:

$$\begin{aligned} & [mVs + 2(K_f + K_r)] \beta(s) \\ & + \left[ mV + \frac{2}{V} (l_f K_f - l_r K_r) \right] r(s) \\ & = 2K_r \delta_f(s) \end{aligned} \quad (5)$$

$$\begin{aligned} & 2(l_f K_f - l_r K_r) \beta(s) \\ & + \left[ Is + \frac{2(l_f^2 K_f + l_r^2 K_r)}{V} \right] r(s) \\ & = 2l_f K_f \delta_f(s) \end{aligned} \quad (6)$$

where  $\beta(s)$ ,  $r(s)$ , and  $\delta_f(s)$  are Laplace transform variables of  $\beta$ ,  $r$ , and  $\delta_f$ , respectively. After some manipulation of Eqs. (5) and (6), the following input/output relations can be derived. In this case, steer angle is the input and side slip

angle is the output variable.

$$\frac{\beta(s)}{\delta_f(s)} = \frac{\begin{vmatrix} 2K_f & mV + \frac{2}{V}(l_f K_f - l_r K_r) \\ 2l_f K_f & Is + \frac{2}{V}(l_f^2 K_f + l_r^2 K_r) \end{vmatrix}}{\begin{vmatrix} mVs + 2(K_f + K_r) & mV + \frac{2}{V}(l_f K_f - l_r K_r) \\ (l_f K_f - l_r K_r) & Is + \frac{2}{V}(l_f^2 K_f + l_r^2 K_r) \end{vmatrix}} \quad (7)$$

Generally, when the governing equations of the mechanical system are given, the response for the steer angle can be obtained under adequate driving conditions. The characteristic equations of the system can be easily obtained by setting the denominator of Eq. (7) to zero. Finally, the form of the characteristic equation for this case is:

$$s^2 + 2\zeta\omega_n s + \omega_n^2 = 0 \quad (8)$$

where

$$2\zeta\omega_n = \frac{2m(l_f^2 K_f + l_r^2 K_r) + 2I(K_f + K_r)}{mIV} \quad (9)$$

$$\omega_n^2 = \frac{4K_f K_r l^2}{mIV^2} - \frac{2(l_f K_f - l_r K_r)}{I} \quad (10)$$

In Eq. (10),  $l$  is the wheel base of the vehicle ( $l_f + l_r$ ). If  $\omega_n$  is the a natural frequency and  $\zeta$  is the damping ratio for the lateral vehicle dynamics, the final forms of these terms are obtained as follows:

$$\omega_n = \frac{2l}{V} \sqrt{\frac{K_f K_r}{mI}} \sqrt{1 + SF \cdot V^2} \quad (11)$$

$$\zeta = \frac{m(l_f^2 K_f + l_r^2 K_r) + I(K_f + K_r)}{2l \sqrt{mIK_f K_r} (1 + SF \cdot V^2)} \quad (12)$$

These represent basic characteristics of an automobile in lateral vehicle dynamics with respect to the steering input. Like the conventional meaning of natural frequency and damping ratio, these are used as a standard for the lateral motion of the system. In Eqs. (11) and (12),  $SF$  is the stability factor of the vehicle and is expressed as follows:

$$SF = -\frac{m}{2l^2} \frac{l_f K_f - l_r K_r}{K_f K_r} \quad (13)$$

This term is known as the understeer/oversteer gradient. If a vehicle has a positive value of  $SF$ , it shows an understeer characteristic. Like Eqs. (11) and (12), the natural frequency and

damping ratio are functions of the design variables and speed of the vehicle.

Finally, the transfer function between steering angle input and side slip angle output can be expressed with the previous information: it is a function of the vehicle design variables and some basic vehicle functions ( $SF$ ,  $\zeta$ , and  $\omega_n$ ). Since our major concern is on the response of the side slip angle in the frequency domain, the following transfer function can be obtained from Eq. (7):

$$\begin{aligned} G_{\delta}^{\beta}(s) &= \frac{\beta(s)}{\delta_f(s)} \\ &= G_{\delta}^{\beta}(0) \cdot \frac{1 + T_{\beta}s}{1 + \frac{2\zeta}{\omega_n}s + \left(\frac{1}{\omega_n}\right)^2 s^2} \end{aligned} \quad (14)$$

where

$$G_{\delta}^{\beta}(0) = \frac{1 - \frac{m}{2l} \frac{l_f}{l_r K_r} V^2}{1 + SF \cdot V^2} \cdot \frac{l_r}{l} \quad (15)$$

$$T_{\beta} = \frac{IV}{2l_r K_r} \frac{1}{1 - \frac{m}{2l} \frac{l_f}{l_r K_r} V^2} \quad (16)$$

Here  $T_{\beta}$  is the coefficient of  $s$  in the numerator of the transfer function, and  $G_{\delta}^{\beta}(0)$  is the side slip angle gain defined as the ratio of the side slip angle with respect to the front wheel steering angle when the vehicle is in the steady circular turning maneuver.

It is noted that  $T_{\beta}$  has two distinct values as the vehicle speed increases. In the low speed range, the value of  $T_{\beta}$  is positive. Otherwise,  $T_{\beta}$  has negative values in high speed regions. It means that a transition speed,  $V_{\beta}$ , exists in the side slip response, and is easily obtained from Eq. (16) and the exact mathematical form is derived as follows:

$$V_{\beta} = \frac{2l_r K_r}{ml_f} \quad (17)$$

$V_{\beta}$  is the speed of the vehicle and is a function of the vehicle parameters. At this speed, the gain of the transfer function for the side slip angle has zero value. This point might be treated as a transition point of the side slip angle response of the vehicle. Because of this point, the response characteristics of the side slip angle are classified into two distinct domains. Under the transition

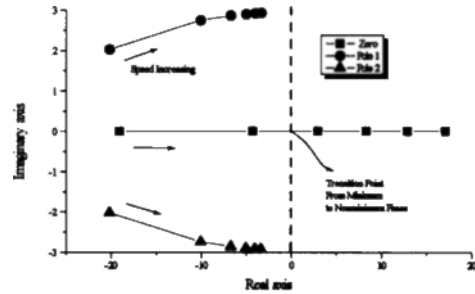


Fig. 2 Pole-zero map w.r.t. the change of vehicle speed

speed, the zero of the system is located in the left-half plane in the  $s$ -plane. It means that the zero dynamics is stable at this speed range. Otherwise, the zero dynamics is unstable due to the right-half plane zero at above-transition speeds. Therefore, we can say that the characteristics of the system are changed from minimum phase to non-minimum phase as the vehicle speed increases (Ogata, 1990, Franklin *et al.*, 1994). This will occur in the side slip angle gain of Eq. (15). In order to explain the above phenomenon, the pole-zero map with respect to the change of vehicle speed is suggested in Fig. 2.

### 3. Formulation for the Sensitivity Analysis

In this chapter, sensitivity functions on the side slip angle with respect to the design variables are derived. These could be classified into sensitivity functions for the basic terms and magnitude and phase of the transfer function for the more systematic approach.

#### 3.1. Sensitivity functions for the basic terms

For the formulation of the sensitivity functions for the side slip angle with respect to the design variables, sensitivity formulations for the basic functions are performed at the initial stage. This information is useful for derivation of the sensitivity of magnitude and phase of the transfer function. The sensitivity formulations are summarized in Table 1.

**Table 1** Basic functions and sensitivity functions

Basic functions	Sensitivity functions
$SF$	$\frac{\partial SF}{\partial b}$
$\omega_n$	$\frac{\partial \omega_n}{\partial b}$
$\zeta$	$\frac{\partial \zeta}{\partial b}$

The basic functions for the vehicle can be defined as a function of the vehicle parameters. A sensitivity function for the basic functions is the partial derivative of the functions with respect to the design variable vector (Jang, 1995b). This sensitivity information for damping ratio, natural frequency, and stability factor will be used for formulation of the magnitude and phase of the transfer functions.

### 3.2. Sensitivity functions for the magnitude and phase

From Eq. (14), sensitivity functions for the magnitude and phase of the transfer function can be derived. Contents of the previous section are used for the systematic derivation process. First, magnitude and phase of the transfer function are defined as follows. In order to check the frequency response, Laplace variables have to be replaced by the following terms  $s = j2\pi f$ . In this case,  $f$  is the forcing input frequency (Hz) to the vehicle, and  $j$  indicates the imaginary part of the complex variable. Therefore, the magnitude of the transfer function is:

$$|G_s^g(j2\pi f)| = A \cdot B \quad (18)$$

where

$$A = |G_s^g(0)|,$$

$$B = \sqrt{\frac{P_\beta^2 + Q_\beta^2}{R_\beta^2 + S_\beta^2}}.$$

The phase of the transfer function is:

$$\angle G_s^g(j2\pi f) = \tan^{-1}\left(\frac{Q_\beta}{P_\beta}\right) - \tan^{-1}\left(\frac{S_\beta}{R_\beta}\right) \quad (19)$$

where  $P_\beta$ ,  $Q_\beta$ ,  $R_\beta$  and  $S_\beta$  are defined as follows:

$$P_\beta = 1$$

$$Q_\beta = T_\beta(2\pi f)$$

$$R_\beta = 1 - \left(\frac{2\pi f}{\omega_n}\right)^2$$

$$S_\beta = 2\frac{\zeta}{\omega_n}(2\pi f) \quad (20)$$

As the first process of the derivation of the sensitivity functions in the frequency domain, sensitivity of the magnitude must be considered. If we perform the partial differentiation of the magnitude with respect to the design variables, the following general sensitivity function for magnitude can be obtained from Eq. (18):

$$\frac{\partial}{\partial b} |G_s^g(j2\pi f)| = A_{\underline{b}} \cdot B + A \cdot B_{\underline{b}} \quad (21)$$

where  $A_{\underline{b}}$  and  $B_{\underline{b}}$  are partial derivatives of  $A$  and  $B$  with respect to the design variable vector  $\underline{b}$ . For the evaluation of the sensitivity functions for magnitude, let us divide Eq. (21) into parts. In order to determine the sensitivity of  $A$  in Eq. (21) with respect to the design variables, the side slip angle gain coefficient can be re-defined from Eq. (15):

$$A = f_A(\underline{b}) \cdot g_A(\underline{b}) \quad (22)$$

where

$$f_A(\underline{b}) = \left| 1 - \frac{m}{2l} \frac{l_f}{l_r K_r} V^2 \right|,$$

$$= \begin{cases} 1 - \frac{m}{2l} \frac{l_f}{l_r K_r} V^2, & (\text{at } V < V_\beta) \\ \frac{l}{2l} \frac{l_f}{l_r K_r} V^2 - 1, & (\text{at } V > V_\beta) \end{cases}$$

$$g_A(\underline{b}) = \frac{l_r}{(1 + SF \cdot V^2) l}.$$

Finally, the sensitivity of  $A$  with respect to the design variables is derived. The exact expressions of the sensitivity functions for the sub-functions have been summarized in Ref. (Jang, 1995b):

$$A_{\underline{b}} = \frac{\partial}{\partial b} [f_A \cdot g_A] = \frac{\partial f_A}{\partial b} g_A + f_A \frac{\partial g_A}{\partial b} \quad (23)$$

The sensitivity function of  $B$  in Eq. (21) with respect to the design variables is obtained as follows:

$$B_{\underline{b}} = \frac{1}{2} \sqrt{\frac{R_\beta^2 + S_\beta^2}{P_\beta^2 + Q_\beta^2}} \cdot \frac{\partial}{\partial b} \left( \frac{P_\beta^2 + Q_\beta^2}{R_\beta^2 + S_\beta^2} \right) \quad (24)$$

where

$$\frac{\partial}{\partial b} \left( \frac{P_\beta^2 + Q_\beta^2}{R_\beta^2 + S_\beta^2} \right) = \frac{\left( \left[ \frac{\partial}{\partial b} (P_\beta^2 + Q_\beta^2) \right] (R_\beta^2 + S_\beta^2) - (P_\beta^2 + Q_\beta^2)^2 \left[ \frac{\partial}{\partial b} (R_\beta^2 + S_\beta^2) \right] \right)}{(R_\beta^2 + S_\beta^2)^2} \quad (25)$$

with

$$\frac{\partial}{\partial b} (P_\beta^2 + Q_\beta^2) = 2P_\beta \frac{\partial P_\beta}{\partial b} + 2Q_\beta \frac{\partial Q_\beta}{\partial b} \quad (26)$$

$$\frac{\partial}{\partial b} (R_\beta^2 + S_\beta^2) = 2R_\beta \frac{\partial R_\beta}{\partial b} + 2S_\beta \frac{\partial S_\beta}{\partial b} \quad (27)$$

where the partial derivatives of  $P_\beta$ ,  $Q_\beta$ ,  $R_\beta$ , and  $S_\beta$  with respect to the design variables are defined as follows:

$$\begin{aligned} \frac{\partial P_\beta}{\partial b} &= 0 \\ \frac{\partial Q_\beta}{\partial b} &= (2\pi f) \frac{\partial T_\beta}{\partial b} \\ \frac{\partial R_\beta}{\partial b} &= (2\pi f)^2 \frac{2}{\omega_n^3} \frac{\partial \omega_n}{\partial b} \\ \frac{\partial S_\beta}{\partial b} &= (4\pi f) \frac{\partial}{\partial b} \left( \frac{\zeta}{\omega_n} \right) \end{aligned} \quad (28)$$

The sensitivity function for  $T_\beta$  can be derived by partial differentiation of  $T_\beta$  with respect to the design variables. Also, the exact expressions of the sensitivity function for the sub-functions have been summarized in Ref. (Jang, 1995b).

As the second step of the derivation of the sensitivity functions in the frequency domain, sensitivity of the phase must be considered. The sensitivity function for the phase function can be obtained by partial differentiation of the function with respect to the design variables:

$$\frac{\partial}{\partial b} \angle G_\beta^\beta = \left[ \frac{P_\beta^2}{P_\beta^2 + Q_\beta^2} \right] \frac{\partial}{\partial b} \left( \frac{Q_\beta}{P_\beta} \right) - \left[ \frac{R_\beta^2}{R_\beta^2 + S_\beta^2} \right] \frac{\partial}{\partial b} \left( \frac{S_\beta}{R_\beta} \right) \quad (29)$$

where

$$\frac{\partial}{\partial b} \left( \frac{Q_\beta}{P_\beta} \right) = \frac{1}{P_\beta^2} \left[ \frac{\partial Q_\beta}{\partial b} \cdot P_\beta - Q_\beta \cdot \frac{\partial P_\beta}{\partial b} \right] \quad (30)$$

$$\frac{\partial}{\partial b} \left( \frac{S_\beta}{R_\beta} \right) = \frac{1}{R_\beta^2} \left[ \frac{\partial S_\beta}{\partial b} \cdot R_\beta - S_\beta \cdot \frac{\partial R_\beta}{\partial b} \right] \quad (31)$$

The partial derivatives of  $P_\beta$ ,  $Q_\beta$ ,  $R_\beta$ , and  $S_\beta$  are derived from Eq. (28). As a result, Eqs. (21) ~ (31) are used for all sensitivity analyses in the frequency domain.

## 4. Results of the Sensitivity Analysis

Various sensitivity analyses were carried about a nominal point for the front wheel vehicle system in the frequency domain. Vehicle data used in this research are listed in Table 2. These data are general for conventional mid-size passenger cars. From these data, we see that the car shows understeer characteristics and directional stability for steering maneuver.

**Table 2** Vehicle data list used for analysis

Design variable	Data	Dimension
$m$	1,300	kg
$I$	2,100	kg·m <sup>2</sup>
$K_f$	40,000	N/rad
$K_r$	30,000	N/rad
$l_f$	1.01	m
$l_r$	1.65	m

Sensitivity information is evaluated in various vehicle speed ranges (20km/h~120km/h) with respect to the design variables. Initially, the effects of each design variable for the side slip angle are examined. Secondly, a dominant design variable is checked by comparison of the results. Before the sensitivity analysis, conventional frequency analyses are performed for the magnitude and phase of the side slip angle with respect to various vehicle speeds. The results of the magnitude and

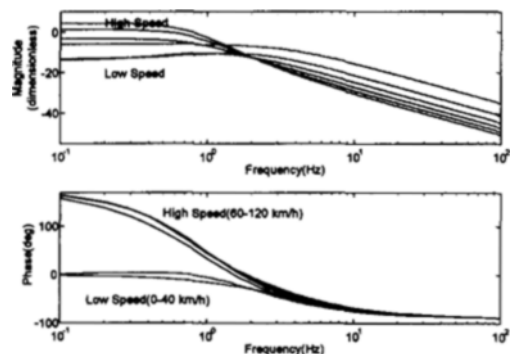


**Fig. 3** Magnitude and phase change of the side slip angle w.r.t. vehicle speed (km/h)

phase analysis angle are presented in Fig. 3. From these results, we see that the magnitude and phase of the side slip angle change irregularly with variations in vehicle speed.

In view of the magnitude for side slip angle, under 1~2 Hz, it decreases until the vehicle speed reaches 60km/h. However it increases above this speed. Otherwise, above 1~2 Hz region it decreases as the vehicle speed increases. In the case of phase for side slip angle, under 3 Hz, it increases as the vehicle speed increases. Above 60km/h, phase lead quantity is detected. Since the zero of the side slip angle is located in the right-half plane within the speed range, we can conclude that the zero dynamics is unstable. This means that the system has non-minimum phase (Ogata, 1990, Franklin *et al.*, 1994). From this research, we conclude that this phenomenon occurs when the vehicle speed is above the transition speed  $V_{\beta}$  in Eq. (16). Also, we suggest that this speed must be treated as an important criterion for the frequency response of the side slip angle. Otherwise, above 3 Hz the phases for all speed ranges converge to  $-90^{\circ}$ . From the trends of magnitude and phase of the side slip angle, we conclude that the frequency responses of the side slip angle are dominant under the 1 Hz region.

#### 4.1 The effects of the vehicle mass

The effects of vehicle mass on the magnitude and phase of the side slip angle are considered in the frequency domain. Figure 4 shows the results of the side slip angle sensitivity with respect to

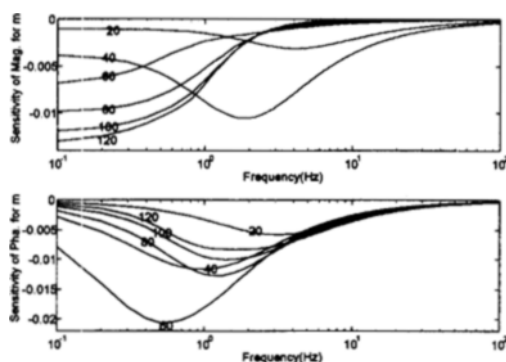


Fig. 4 Side slip angle sensitivity for  $m$  w.r.t. change in vehicle speed (km/h)

change in vehicle mass. The upper figure shows that the magnitude sensitivity of the side slip angle with respect to the vehicle mass decreased until 0.3 Hz as the vehicle speed increased. In the 0.3~0.8 Hz region, the sensitivity values have different trends compared to the values for under 0.3 Hz. An interesting observation from this result is that the sensitivity value of magnitude for vehicle mass has a maximum at about 2 Hz with 40 km/h vehicle speed. After 2 Hz region, all values converge to zero. The lower figure shows the results of the phase sensitivity with respect to the vehicle mass according to the speed change. In this result, the values for low speed (20~60km/h) decrease as the speed increases for under 1 Hz. But in the same frequency region, the values for high speeds (60~120km/h) increase. The value for 60km/h has a maximum in the same region. Like the case of sensitivity for magnitude, the values converge to the zero as the frequency is increased.

#### 4.2 The effects of the vehicle inertia

The effects of the vehicle inertia in the yaw direction to the side slip angle are studied in the frequency domain. Figure 5 shows the results of the side slip angle sensitivity with respect to changes in vehicle inertia. In the upper figure, the value for 20 km/h vehicle speed is very small, and the values for 40 km/h and 60 km/h are positive. Otherwise, the values for the high speeds (80~120km/h) decrease as speed is increased. From this result, we see that the sensitivity value of

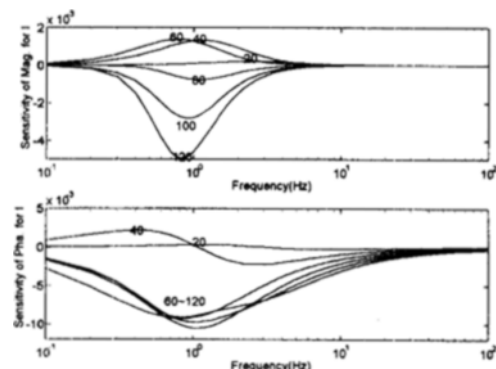


Fig. 5 Side slip angle sensitivity for  $I$  w.r.t. change of vehicle speed (km/h)

magnitude with respect to the vehicle inertia is dominant in the 1 Hz range. In the lower figure, the sensitivity of the phase is represented. In the 40 km/h vehicle speed, a zero point of the sensitivity value is detected at about 1 Hz. The side slip angle may have maximum value at this point. Therefore it must be carefully examined. Usually, we can say that a vehicle has an uncertain dynamic nature at this point.

#### 4.3 The effects of the cornering stiffness of the front wheel

The effects of cornering stiffness of the front wheel to the side slip angle are considered in the frequency domain. Figure 6 shows the side slip angle sensitivity with respect to changes in cornering stiffness of the front wheel. The sensitivity of the magnitude and phase are shown in the upper and lower parts of Fig. 6, respectively. In the range of 0~40km/h vehicle speed, the sensitivity values for magnitude are positive, while above this speed range the value of sensitivity decreases as the vehicle speed increased. Any zero points of the sensitivity value do not exist in this case. As the vehicle speed increased, the maximum sensitivity point is located under 1 Hz. In case of the sensitivity for the phase, all trends are the same as the magnitude case under 1 Hz. However, above 60 km/h, the zero points of the sensitivity value are detected at about 1 Hz. Above 1 Hz, the sensitivity values for phase decrease as the vehicle speed increased. As the frequency continuously increases, all sensitivity values converge to the

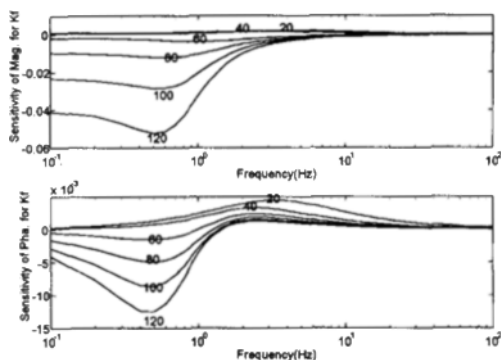


Fig. 6 Side slip angle sensitivity for  $K_f$  w.r.t. the change of vehicle speed (km/h)

zero value. It must be noted that the response of the sensitivity for phase is dominant in the frequency range of 1~1.5 Hz.

#### 4.4 The effects of cornering stiffness on the rear wheel

The effects of cornering stiffness on the rear wheel to the side slip angle are analyzed in the frequency domain. Figure 7 shows the results of the side slip angle sensitivity with respect to changes in the cornering stiffness of the rear wheel. The sensitivity values of side slip angle for cornering stiffness of the front wheel increase as the vehicle speed increased. Any zero points of the sensitivity value do not exist in this case. Under 60 km/h, the trends of the value are somewhat ambiguous. But above this speed, the trends of the value are explicitly represented in the upper figure. Also, under the 1 Hz region, these trends are explicitly represented but, above 1 Hz, it is not explicit. In the lower figure, the sensitivity values of the phase are shown. The values increase as the vehicle speeds increased until the speed reaches 60 km/h. Otherwise, above 60 km/h, the sensitivity values continuously decrease as the vehicle speed increased. Like the previous case, all maximum sensitivity values occurred near the 1 Hz region. In this case zero points of the sensitivity value do not exist.

#### 4.5 The effects of the distance from c. g. to front wheel center

The effects of the distance from center of grav-

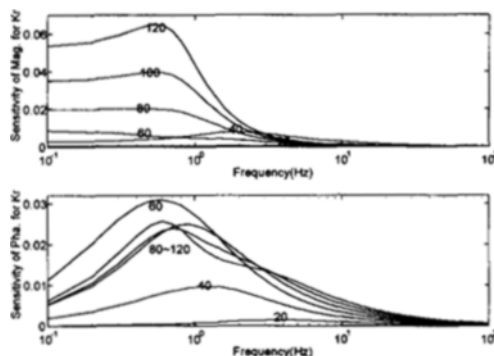
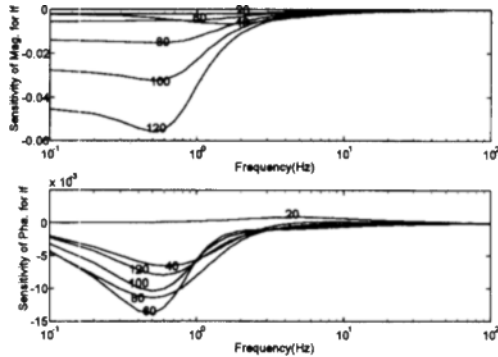


Fig. 7 Side slip angle sensitivity for  $K_r$  w.r.t. the change of vehicle speed (km/h)



**Fig. 8** Side slip angle sensitivity for  $l_f$  w.r.t. the change of vehicle speed (km/h)

ity to front wheel center to the side slip angle are considered in the frequency domain. Figure 8 shows the results of the side slip angle sensitivity with respect to changes in distance from center of gravity to front wheel center. In this case, the values increase as the vehicle speed increased. Any zero points of the sensitivity value do not exist in this case. Under 60 km/h, the trends of the value are somewhat ambiguous. But above this speed, the trends of the value are explicitly represented in the upper figure. Also, under the 1 Hz region, these trends are explicitly represented but, above 1 Hz, it is not explicit. In the lower figure, the sensitivity values of the phase are shown. The values increase as the vehicle speed increased until 60 km/h. Otherwise, in the 80 ~ 100 km/h speed range, the sensitivity value has a small value compared to the value of the value for 60 km/h. Above these speed range, the values continuously decreased as the vehicle speed increased. Like the previous case, all maximum sensitivity values occurred near the 1 Hz. In this case, zero points of the sensitivity value do not exist.

#### 4.6 The effects of the distance from c. g. to rear wheel center

The effects of the distance from center of gravity to rear wheel center to the side slip angle are studied in the frequency domain. The result of the side slip angle sensitivity with respect to change of the distance from center of gravity to rear wheel center is shown in Fig. 9. In this case, the values

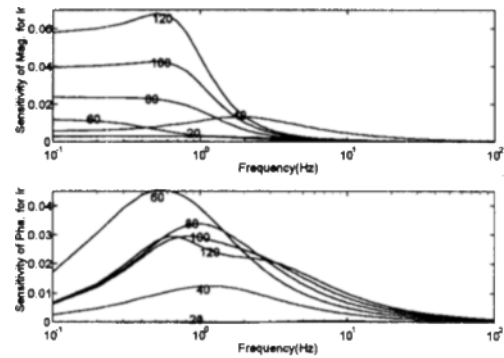


**Fig. 9** Side slip angle sensitivity for  $l_r$  w.r.t. the change of vehicle speed (km/h)

increase as the vehicle speed increased. Any zero points of the sensitivity value are not detected. Like the previous case, the trends of the value are more or less ambiguous under 60 km/h. But above this speed, the trends of the value are explicitly represented in the upper figure. Also under the 1 Hz region, these trends are explicitly represented but, above the 1 Hz, it is not explicit. In the lower figure, the sensitivity values of the phase are suggested. The values positively increased as the vehicle speed increased until 60 km/h. Otherwise, above the 60 km/h, the sensitivity values continuously decreased as the vehicle speed increased. Like the previous case, all maximum sensitivity values occurred near the 1 Hz. In this case, we can not find any zero points of the sensitivity value.

#### 4.7 Dominant design variable study

The dominant design variables can be examined based on the sensitivity analyses for side slip angle of the vehicle at the center of gravity. In order to check the dominant design variable, a normalization process is required for dimension matching. In this research, 1% perturbation of the design variables is performed for this process. The rank of the design variables is different depending on the vehicle speed. In this study, only two vehicle speeds (40 km/h and 80 km/h) are considered.

In case of 40 km/h vehicle speed, the results are grouped in Fig. 10. From the upper figure, we can see that a dominant design variable for magnitude

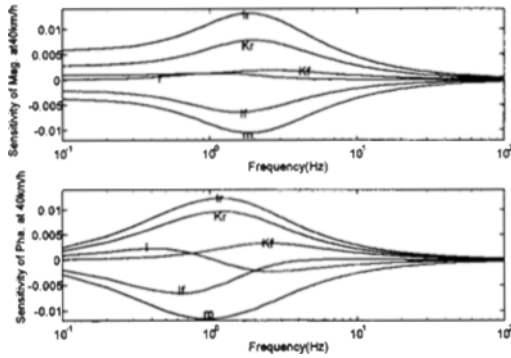


**Fig. 10** Side slip angle sensitivity w.r.t. each design variables at 40km/h

of the side slip angle is  $l_r$ . Next, we consider,  $m$ ,  $l_f$ ,  $K_r$ ,  $K_f$ , and  $I$ . The sensitivities have quite different values at about 2 Hz. But as the frequency increases, the values converge to zero. Zero points are not detected at this vehicle speed. From the lower figure, we can see that a dominant design variable for phase of the side slip angle is  $l_r$ . Next,  $m$ ,  $K_r$ ,  $l_f$ ,  $K_f$ , and  $I$  are followed in turn. In this case, the sensitivities have mostly different values at around 1 Hz. Also, in spite of  $I$  having lower value for phase sensitivity, it must be carefully treated at the analysis and control stage, because it has zero sensitivity value at about 1 Hz. In this point, the phase of the side slip angle may have maximum value. However, the values of the high frequency converge to zero as in the magnitude case.

In case of 80 km/h vehicle speed, the results are shown in Fig. 11. Like the previous magnitude results, we see that a dominant design variable for magnitude is  $l_r$ . Next,  $K_r$ ,  $l_f$ ,  $K_f$ ,  $m$ , and  $I$  are followed in turn. The sensitivities have quite different values at about 1 Hz. But as the frequency is increased, the values are converge to zero. Any zero points are not detected at this vehicle speed. From the lower figure, we can see that a dominant design variable for phase of the side slip angle is  $l_r$ . Next,  $K_r$ ,  $m$ ,  $I$ ,  $l_f$ , and  $K_f$  are followed in turn. In this case, the sensitivities have mostly different values near 1 Hz. Also, in spite of  $K_f$  has a lower value for phase sensitivity, it must be carefully treated at the analysis and control stage, because it has zero sensitivity value near 1.

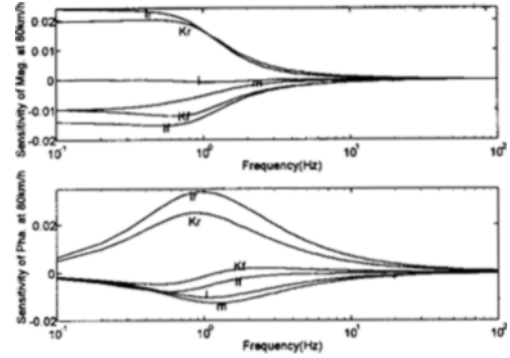


**Fig. 11** Side slip angle sensitivity w.r.t. each design variables at 80km/h

2 Hz. However, the values of the high frequency converge to zero like in the magnitude case.

From Fig. 10 and Fig. 11, we can conclude that the sensitivity variables for design variables are changed as the vehicle speed changes. For example, the vehicle mass effect is reduced as the vehicle speed increased. Also, the effect of vehicle inertia to the sensitivity of the phase increases as the vehicle speed increased. This change point of the vehicle response is detected in this study at about 1 Hz. This could be used as a basis for the development of a vehicle that has more enhanced frequency response for handling performance, as well as new-robust control for external disturbances. Also, this may be used by vehicle the designer for either re-design or initial design of the vehicle.

## 5. Conclusions

In this study, the sensitivity analyses for the side slip angle of the front wheel steering vehicle system are carried out in the frequency domain. From various sensitivity analyses, useful sensitivity information is evaluated at various vehicle speeds with respect to the design variables. First, the effects of each design variable on the state variables are examined. Secondly, a dominant design variable is checked by comparison of the results. In these results, zero points of the state sensitivity variable which may be a critical point for vehicle design and control are detected. These points must be carefully considered as a design

base. Also, we see that the effects on state sensitivity of the distance from center of gravity to rear wheel center, and from center of gravity to front wheel center, are the most sensitive design variables. Also, the vehicle mass has the second highest sensitivity at low speed ranges. But its importance is continuously reduced as the vehicle speed increased. In the case of vehicle control, the zero points of the state sensitivity results must be outside the nominal driving conditions because severe problems may occur at these points. In the case of vehicle design, a modification of the vehicle wheel base must be carefully addressed for a reasonable vehicle design. Also, we find that the frequency response of the side slip angle has two distinct characteristics. These two distinct domains are divided into stable and unstable zero dynamics regions. This means that the characteristics are changed from minimum phase to non-minimum phase as the vehicle speed increased due to the change in zero dynamics. We also see that the dominant frequency range goes down as the speed increased. Therefore, a vehicle must be considered separately at various vehicle speeds. This research may be used for design optimization in the frequency domain, and for controller design of the vehicle.

## References

- Arora, J. S., 1989, *Introduction to Optimum Design*, McGraw-Hill International Editions
- Chang, C. O. and Nikravesh, P. E., 1985, "Optimal Design of Mechanical Systems with Constraint Violation Stabilization Method," *Journal of Mechanisms, Transmissions, and Automation in Design*, Vol. 107, pp. 493~498.
- Deif, A. S., 1986, *Sensitivity Analysis in Linear Systems*, Springer-Verlag, Berlin, Heidelberg
- Ellis, J. R., 1969, *Vehicle Dynamics*, London Business Book Ltd., London
- Franklin, G. F., Powell, J. D., and Emami-Naeini, A., 1994, *Feedback Control of Dynamic Systems*, 3rd ed., Addison-Wesley Publishing Company, Inc.
- Gillespie, T. D., 1992, *Fundamentals of Vehicle Dynamics*, Society of Automotive Engineers, Inc.
- Haug, E. J., Mani, N. K. and Krishnaswami, P., 1984, "Design Sensitivity Analysis and Optimization of Dynamically Driven Systems," *Computer Aided Analysis and Optimization of Mechanical System Dynamics, NATO ASI Series F: Computer and Systems Sciences*, Vol. 9, pp. 555~636.
- Haug, E. J. and Sohoni, V. N., 1984, "Design Sensitivity Analysis and Optimization of Kinematically Driven Systems," *Computer Aided Analysis and Optimization of Mechanical System Dynamics, NATO ASI Series F: Computer and Systems Sciences*, Vol. 9, pp. 499~554
- Jang, J. H., 1995a, *Note for Vehicle Dynamics and Control*, Ed. 1, in Korean
- Jang, J. H., 1995b, *The Sensitivity Analysis for the Front Wheel Steering Vehicle*, Technical Report No. 95-2, Center for Car & Robotics, The University of Hanyang
- Jang, J. H., Jeong, W. S., and Han, C. S., 1995, "Modeling and Dynamic Analysis for Four Wheel Steering Vehicle," *Korea Society of Automotive Engineers*, SAE No. 953737
- Jang, J. H. and Han, C. S., 1995, "The State Sensitivity Analysis of the Front Wheel Steering Vehicle: In the Time Domain," is submitted to *KSME International Journal*
- Jang, J. H. and Han, C. S., 1997, "The Sensitivity Analysis of Yaw Rate for a Front Wheel Steering Vehicle: In the Frequency Domain," *KSME International Journal*, Vol. 11, No. 1, pp. 56~66
- Jansen, S. T. H. and van Oosten, J. J. M., 1994, "The Development and Evaluation of an Active 4WS Vehicle Simulation Model with Limited Complexity using Driving Tests," *AVEC '94*, 9438664, pp. 438~443
- Krishnaswami, P., Wehage, R. A., and Haug, E. J., 1983, *Design Sensitivity Analysis of Constrained Dynamic Systems by Direct Differentiation*, Technical Report No. 83-5, Center for Computer Aided Design, The University of Iowa
- Ogata, K., 1990, *Modern Control Engineering*, 2nd ed., Prentice-Hall International Editions
- Shiotsuka, T., Nagamatsu, A., and Yoshida, K., 1993, "Adaptive Control of 4WS System by Using

Neural Network," *International Journal of Vehicle Mechanics and Mobility, Vehicle System Dynamics*, Vol. 22, No. 5-6, pp. 411~424

Slotine, J. E. and Li, W., 1991, *Applied Non-linear Control*, Prentice-Hall

Vanderplaats, G. N., 1984, *Numerical Optim-*

*ization Techniques for Engineering Design with Applications*, McGraw-Hill, New York

Whitehead, J. C., 1988, "Four Wheel Steering: Maneuverability and High Speed Stabilization," *Society of Automotive Engineers, Inc.*, SAE 880642, pp. 668~679